Interphotoreceptor Retinoid-Binding Protein Is the Physiologically Relevant Carrier That Removes Retinol from Rod Photoreceptor Outer Segments†

Qingqing Wu,‡,§ Lorie R. Blakeley,‡ M. Carter Cornwall,|| Rosalie K. Crouch,‡ Barbara N. Wiggert,⊥ and Yiannis Koutalos*,‡

Department of Ophthalmology, Medical University of South Carolina, Charleston, South Carolina, Department of Nephrology, First Affiliated Hospital of Sun Yat-sen University, Guangzhou, P.R. China, Department of Physiology and Biophysics, Boston University School of Medicine, Boston, Massachusetts, and Laboratory of Retinal Cell and Molecular Biology, National Eye Institute, Bethesda, Maryland

Received March 7, 2007; Revised Manuscript Received May 22, 2007

ABSTRACT: Light detection by vertebrate rod photoreceptor outer segments results in the destruction of the visual pigment, rhodopsin, as its retinyl moiety is photoisomerized from 11-*cis* to all-*trans*. The regeneration of rhodopsin is necessary for vision and begins with the release of the all-*trans* retinal and its reduction to all-*trans* retinol. Retinol is then transported out of the rod outer segment for further processing. We used fluorescence imaging to monitor retinol fluorescence and quantify the kinetics of its formation and clearance after rhodopsin bleaching in the outer segments of living isolated frog (*Rana pipiens*) rod photoreceptors. We independently measured the release of all-*trans* retinal from bleached rhodopsin in frog rod outer segment membranes and the rate of all-*trans* retinol removal by the lipophilic carriers interphotoreceptor retinoid binding protein (IRBP) and serum albumin. We find that the kinetics of all-*trans* retinol formation in frog rod outer segments after rhodopsin bleaching are to a good first approximation determined by the kinetics of all-*trans* retinal release from the bleached pigment. For the physiological concentrations of carriers, the rate of retinol removal from the outer segment is determined by IRBP concentration, whereas the effect of serum albumin is negligible. The results indicate the presence of a specific interaction between IRBP and the rod outer segment, probably mediated by a receptor. The effect of different concentrations of IRBP on the rate of retinol removal shows no cooperativity and has an EC_{50} of 40 μmol/L.

The vertebrate cells responsible for vision are the rod and cone photoreceptors of the retina that convert incoming light to an electrical signal. This conversion takes place in the photoreceptor outer segments, which are full of membrane disks containing the visual pigment, and, in a physiologically important arrangement, are enveloped by the retinal pigment epithelium (RPE). The visual pigment is composed of a chromophore, 11-*cis* retinal, attached to an integral membrane protein, opsin. The detection of light begins with the absorption of incoming photons by the visual pigment. An absorbed photon isomerizes the chromophore moiety from 11-*cis* to all-*trans*, bringing about a conformational change that initiates a cascade of reactions culminating in membrane potential change. The recovery of the cell from light involves the deactivation of the intermediates activated by light and the reestablishment of membrane potential (*1*, *2*). However, the isomerized chromophore, all-*trans* retinal, remains. For vision to be possible, it is essential that the visual pigment regenerates: that is, the all-*trans* retinal has to be removed, and fresh 11-*cis* retinal has to be provided to combine with opsin and reform the visual pigment. The reactions regenerating the pigment are known as the Visual Cycle (*3*−*5*).

In the case of the rod photoreceptors, the cells responsible for vision at low light intensities, the Visual Cycle encompasses reactions in the outer segment and in the adjacent RPE cells. The first step in the Cycle is the release of all-*trans* retinal from photoactivated rhodopsin after hydrolysis of the Schiff base bond linking the chromophore to opsin. All-*trans* retinal is then reduced to all-*trans* retinol in a reaction catalyzed by retinol dehydrogenase (*6*, *7*), requiring NADPH and taking place on the cytoplasmic side of the outer segment disks. It is possible that all-*trans* retinal ends up inside the disks, bound via a Schiff base to phosphatidylethanolamine, in which case the phosphatidylethanolamine-all-*trans*-retinal compound is transported to the cytoplasmic side by the ABCR transporter (*8*−*10*), making all-*trans* retinal available for reduction. The all-*trans* retinol formed in the rod outer segment is transported to the RPE, in a process that can be facilitated by the interphotoreceptor retinoid-binding protein (IRBP[1]; (*11*−13)). In the RPE, retinol is converted by lecithin-retinol acyltransferase to retinyl ester (LRAT; (*14*, *15*)), which is isomerized to 11-

† This work was supported by NIH/NEI Grants EY14850 (to Y.K.), EY04939 (to R.K.C.), EY01157 (to M.C.C.), Intramural Research Program Grant Z01EY000070 (to B.N.W.), and EY14793, and an unrestricted grant to MUSC Storm Eye Institute from Research to Prevent Blindness, Inc., New York, NY. R.K.C. is an RPB Senior Scientific Investigator.

* Corresponding author. Tel: (843)-792-9180. Fax: (843)-792-1723. E-mail: koutalo@musc.edu.

‡ Medical University of South Carolina.

§ First Affiliated Hospital of Sun Yat-sen University.

|| Boston University School of Medicine.

⊥ National Eye Institute.

10.1021/bi7004619 CCC: $37.00
Published on Web 06/30/2007

cis retinol (*16*, *17*) by the RPE65 protein (*18*−21). 11-*cis* Retinol is then oxidized to 11-*cis* retinal and transported back to photoreceptor outer segments where it associates with opsin to reform rhodopsin.

Previous work (*22*−*25*) has established that all-*trans* retinol can be monitored in the outer segments of living isolated rod and cone photoreceptors from its distinctive fluorescence. Here, we have taken advantage of two properties of frog rod photoreceptors to actually measure the amounts of all-*trans* retinol produced with quantitative biochemical and physiological methods. One, in contrast to larval salamander photoreceptors that contain two types of chromophores (based on vitamins A_1 and A_2) and in widely varying ratios (*24*), frog rods contain a single, vitamin A_1-based chromophore. Two, the metabolic supply of NADPH is not limiting for the formation of all-*trans* retinol in the case of frog rods (*23*), allowing a simplified analysis and direct comparisons between biochemical and physiological data. This has further allowed us to properly characterize the removal of all-*trans* retinol by different lipophilic carriers. In experiments with purified rod outer segment membranes, whole retinas, and living isolated rods, we have separately measured the different steps involved in all-*trans* retinol formation and removal. On the basis of these measurements, we have calculated the predicted kinetics of retinol formation and removal in rod outer segments and found that they are in close agreement with those measured directly from isolated rod photoreceptors. We also characterized the effect of different concentrations of lipophilic carriers on the removal of all-*trans* retinol and established that for the physiological concentrations of carriers the rate of all-*trans* retinol removal is determined by IRBP concentration. Our results strongly support a specific interaction mediating the removal of all-*trans* retinol by IRBP, perhaps through a receptor on the rod outer segment plasma membrane. Throughout the text, when not specifically designated as the 11-*cis* isomers, unqualified retinal and retinol refer to the all-*trans* forms.

MATERIALS AND METHODS

Grass frogs (*Rana pipiens*) were from NASCO (Fort Atkinson, WI) or Carolina Biologicals (Burlington, NC). All animal procedures were carried out in accordance with protocols approved by the Institutional Animal Care and Use Committee of the Medical University of South Carolina and with the recommendations of the Panel on Euthanasia of the American Veterinary Medical Association. Animals were sacrificed after being dark-adapted for at least 3 h, the eyes were enucleated, and the retinas were excised under infrared light in amphibian Ringer's (in mmol/L: 110 NaCl, 2.5 KCl, 1.6 $MgCl_2$, 1 $CaCl_2$, 5 HEPES, and 5 glucose at pH = 7.55).

For experiments with isolated frog rod photoreceptor cells, a retina was chopped with a razor blade on Sylgard elastomer under Ringer's, and the resultant isolated cells were transferred to 100 μL chambers (glass-bottomed culture dishes from Warner Instruments, Hamden, CT). Fluorescence imaging experiments on isolated frog rod photoreceptor cells were carried out with slight modifications of previous procedures (*23*). Chambers containing dark-adapted cells were placed on the stage of an inverted Zeiss Axiovert 100 microscope (Carl Zeiss, Thornwood, NY) and imaged with a Zeiss 40× Plan Neofluar oil immersion objective lens (N.A. = 1.3). Retinol fluorescence was excited with 360 nm light using a Xenon continuous arc light source from Sutter Instrument Company (Novato, CA), and the fluorescence image (emission >420 nm) was acquired with a Hamamatsu CCD camera (Hamamatsu Photonics, Hamamatsu-City, Japan). Only metabolically competent cells (*23*, *26*) were used for retinol fluorescence imaging experiments. Most of the cells are expected to be the rhodopsin-containing red rods, which comprise the overwhelming majority of the rod population in frog retinas (*27*). Image acquisition and analysis were carried out using the Intelligent Imaging Innovations (Denver, CO) software. The increase in outer segment fluorescence after rhodopsin bleaching is due to retinol (*23*). Fluorescence intensity was measured over defined regions of interest (ROI) contained in the outer segment and background. After correcting for background fluorescence, the value of outer segment fluorescence intensity obtained before rhodopsin bleaching was subtracted from all subsequent values.

Outer segment retinol fluorescence was converted to retinol concentration (in mmol/L) through a calibration procedure using hexane/chloroform droplets containing a concentration c = 435 μmol/L all-*trans* retinol. The hexane/chloroform mixture was obtained by mixing hexane containing 870 μmol/L retinol (Sigma Chemical Company, St. Louis, MO) with an equal volume of chloroform. A small volume (5 μL) of the mixture was injected into amphibian Ringer's (0.5 mL), followed by 5 min of sonication in a bath sonicator. Then, 100 μL of the sonicated mixture was placed in a chamber on the microscope stage to image the droplets. The density of the mixture was higher than water, and the droplets settled on the bottom of the chamber. The usual size of the droplets, 3−4 μm, was slightly smaller than the typical diameter of a frog outer segment, 6−7 μm. If C and F are the outer segment concentration and fluorescence of retinol, whereas c and f are those of the droplets, and d and δ are the diameters of the outer segment and droplets, then $F \propto C \cdot d$, $f \propto c \cdot \delta$, and $C = c(\delta/f)(F/d)$. In practice, δ and f were determined from an average of n = 6 droplets, and C was obtained for every outer segment measurement from F and d. This calibration procedure provides a reasonable means for converting the measured retinol fluorescence from intact cells to retinol concentration because, although the quantum yield of a fluorophore is highly sensitive to its environment, in terms of hydrophobicity, the disk membrane lipid bilayer is similar to the hexane/chloroform mixture. In addition, the bulk of all-*trans* retinol generated after rhodopsin bleaching in frog rod outer segments is free and not tightly associated with binding sites that could affect its fluorescence quantum yield (*28*). Finally, the concentrations of retinol estimated according to the calibration procedure were in good agreement with the concentrations estimated from chromophore extractions (see Figure 5).

For experiments with lipophilic carriers, IRBP and bovine serum albumin (BSA) were used. IRBP was purified from bovine retinas as described (*29*). BSA was fatty-acid-free protein from Sigma Chemical Company (St. Louis, MO). The requisite concentrations of carriers were prepared in amphibian Ringer's and added to the chambers containing

[1] Abbreviations: ROS, rod outer segment; IRBP, interphotoreceptor retinoid-binding protein; BSA, bovine serum albumin; IPM, interphotoreceptor matrix.

the cells from the beginning of an experiment or those 30 min after the bleaching of rhodopsin.

For experiments with ROS membranes, excised frog retinas were placed in a buffer (composition in mmol/L: 60 KCl, 30 NaCl, 2 $MgCl_2$, and 10 HEPES at pH = 7.60; dithiothreitol (DTT) and 4-(2-aminoethyl)-benzenesulfonylfluoride (AEBSF) were added to concentrations of 1 and 0.1 mmol/L) containing 45% sucrose. Subsequent procedures were carried out under dim red light. Frog rod outer segment membranes were purified following the procedure of Fung and Stryer (*30*). The final pellet was washed twice and finally suspended in a buffer containing (in mmol/L) 100 KCl, 1 $MgCl_2$, 1 $CaCl_2$, and 10 HEPES at pH = 7.30 and used for experiments. The kinetics of all-*trans* retinal release from bleached rhodopsin were determined by following the regeneration of pigment with the addition of a 5−10× excess of 11-*cis* retinal as follows: a sample of rod outer segment membranes was bleached by exposure to long wavelength light (>530 nm) for 1 min; 11-*cis* retinal was added immediately after bleaching and mixed; afterward, aliquots were withdrawn at different times to determine the extent of all-*trans* retinal release; an aliquot was solubilized in 1% Ammonyx LO in buffer that also contained 20 mmol/L hydroxylamine to convert all chromophores that were not part of rhodopsin to retinal oximes; and the amount of rhodopsin present was determined by bleaching the solubilized rhodopsin with >530 nm light. This rhodopsin has all been newly formed from the opsin made available by the release of all-*trans* retinal. Thus, the fraction of regenerated rhodopsin is the fraction of released all-*trans* retinal. The procedure is based on the lack of any significant competition between all-*trans* retinal and 11-*cis* retinal binding to opsin (*31*). The kinetics of rhodopsin regeneration from opsin were determined in the same way. Opsin was generated by bleaching rod outer segment membranes with >530 nm light for 1 min in buffer containing 20 mmol/L hydroxylamine, and retinal oximes were partially removed by washing the membranes twice with buffer containing 1% BSA. BSA was then removed by washing the membranes with buffer for three more times using a procedure that also removed the hydroxylamine.

For experiments measuring the formation of retinol with quantitative HPLC of retinoid extracts, isolated retinas were incubated at room temperature in Ringer's. Retinoids were extracted at different times after bleaching the retina with >530 nm light for 1 min with slight modifications of the published procedures (*32*, *33*). A retina was homogenized in 200 μL of 0.2% SDS in 10 mmol/L HEPES at pH 6.5 containing 20 mmol/L hydroxylamine, followed by the addition of 0.5 mL of ethanol, and vortexed. Retinoids were extracted with 2 mL of hexane (twice); the hexane phases were separated by centrifugation, collected in a glass vial, and dried under argon; samples were stored at −80 °C until the HPLC run. Samples were suspended in 200 μL of filtered and degassed mobile phase made of hexanes (HPLC grade), ethyl acetate, dioxane, and octanol (85.4:11.2:2.0:1.4). Chromatography was carried out in Waters HPLC (Waters Corporation, Milford, MA), using a 250 mm × 4.6 mm LiChrospher Silica-60 5 μm HPLC column (Alltech Associates, Inc., Deerfield, IL) with a flow rate of 1.00 mL/min and pressure of 424−470 psi. Absorbance was monitored from 300 to 500 nm using the Waters 996 photodiode array, and retinoid peaks were identified using standards and the absorption spectra. The relative amount of a retinoid in the sample was calculated from the area under its peak and its extinction coefficient. The extinction coefficients used are all-*trans* retinol, 51770 cm^{-1} M^{-1} (325 nm); *syn* all-*trans* retinal oxime, 55600 cm^{-1} M^{-1} (357 nm); *anti* all-*trans* retinal oxime, 51700 cm^{-1} M^{-1} (361 nm) (*34*). The fraction of all-*trans* retinol was calculated from the relative amounts and converted to concentration using a total chromophore outer segment concentration of 2.5 mmol/L (*27*). We estimated the efficiency of the extraction procedure for different retinoids using purified bovine ROS membranes with added all-*trans* retinal and all-*trans* retinol. The extraction efficiencies were all-*trans* retinol, 23%; free all-*trans* retinal, 54%; pigment-bound all-*trans* retinal, 40%; and pigment-bound 11-*cis* retinal, 50%. This difference in extraction efficiencies leads to an underestimation of the fraction of all-*trans* retinol by about a factor of 2 for low fractions and ∼20% for high fractions. We have not corrected the results for the difference in the extraction efficiencies between all-*trans* retinal and all-*trans* retinol because it did not affect the overall time course of retinol formation significantly.

All reagents were of analytical grade. All experiments were carried out at room temperature.

DATA ANALYSIS AND KINETIC MODELS

The scheme underlying the data analysis can be represented as a series of three steps, *A*, *B*, and *C*:

$$\text{rhodopsin} \xrightarrow{h\nu} \text{metarhodopsin} \xrightarrow{A} \text{retinal} \overset{B}{\leftrightarrow} \text{retinol} \xrightarrow{C} \text{bulk solution} \quad (1)$$

Photoisomerization of rhodopsin generates a mixture of photoproducts (designated collectively as metarhodopsin), which then release all-*trans* retinal (step *A*), in an irreversible reaction. Retinal is reduced to retinol by retinol dehydrogenase (step *B*), a reaction that is reversible. Finally, retinol is removed from the rod outer segment to bulk solution (step *C*), a reaction that can be sped up by lipophilic carriers.

The kinetics of step *A* were determined *in vitro*, through the measurement of all-*trans* retinal release from the pigment after bleaching in rod outer segment membranes. If *RAL* is the concentration of released retinal at time *t* and RAL_T the total concentration of released retinal, the release kinetics were described as the sum of two first-order processes

$$RAL = RAL_T(1 - A_1 \cdot e^{-k_1 \cdot t} - A_2 \cdot e^{-k_2 \cdot t}) \quad (2)$$

with A_1 and $A_2 = 1 - A_1$ the relative amplitudes and k_1 and k_2 the rate constants.

For the purposes of the analysis, retinal reduction to retinol catalyzed by retinol dehydrogenase (step *B*) was assumed to be close to thermodynamic equilibrium. This assumption allows a direct link between retinal and retinol concentrations and metabolic activity and is supported by the close agreement between the kinetics of retinal release and those of retinol formation (see Results). The reduction of retinal to retinol utilizes NADPH.

$$\text{retinal} + \text{NADPH} + \text{H}^+ \leftrightarrow \text{retinol} + \text{NADP}^+ \quad (3)$$

If *RAL* and *ROL* are the concentrations of retinal and retinol, and K_{eq} the equilibrium constant, then at thermodynamic equilibrium $K_{eq} = RAL[NADPH][H^+]/ROL[NADP^+]$, and upon rearrangement, $ROL/RAL = [NADPH][H^+]/K_{eq}[NADP^+]$. $[NADPH]/[NADP^+] \sim 0.25$ (*35*), $K_{eq} = 3.3 \times 10^{-9}$ M (*36*), and rod outer segment cytoplasmic pH ~7.3 (*37*), leading to a value for the fraction of released chromophore present as retinol $\beta = 0.79$.

$$\beta = ROL/(RAL + ROL) = 0.79 \quad (4)$$

An implicit assumption used in deriving a value for β was that the $[NADPH]/[NADP^+]$ ratio stays approximately constant. This is independently supported by the match between the kinetics of retinal release and those of retinol formation (see Discussion).

The removal of retinol from the rod outer segment (step *C*) is described as a first-order process. Examining the relevant part of eq 1,

$$\text{retinal} \underset{r_2}{\overset{r_1}{\leftrightarrow}} \text{retinol} \xrightarrow{k_3} \text{bulk solution} \quad (1')$$

with r_1 and r_2 the forward and backward rate constants, respectively, for the retinal to retinol conversion and k_3 the rate constant for retinol removal, we have

$$d[ROL]/dt = -k_3 \cdot ROL + r_1 \cdot RAL - r_2 \cdot ROL \quad (5a)$$

$$d[RAL]/dt = -r_1 \cdot RAL + r_2 \cdot ROL \quad (5b)$$

and adding up eqs 5a and 5b, we get

$$d(ROL + RAL)/dt = -k_3 \cdot ROL \quad (5c)$$

or

$$d[ROL]/dt = -\beta \cdot k_3 \cdot ROL = -K_3 \cdot ROL \quad (6a)$$

and

$$d(ROL + RAL)/dt = -K_3 \cdot (ROL + RAL) \quad (6b)$$

The apparent rate constant for retinol removal, $K_3 = \beta \cdot k_3$, is also the one determined experimentally: lipophilic carriers were added to cells 30 min after the bleaching of rhodopsin; retinol fluorescence was normalized to the value at 35 min; and the removal rate was determined by fitting the normalized fluorescence values, $N(t)$, obtained after 35 min, with single-exponential functions of unitary amplitude at $t = 35$ min.

$$N(t) = e^{-K_3 \cdot (t-35)} \quad (7)$$

This mathematical description of the removal process assumes that retinol is eventually fully removed from the outer segment. This was directly observed at high IRBP concentrations, and it was consistent with the decay of retinol fluorescence with time at lower carrier concentrations too. In the absence of carriers, the fluorescence of retinol did not start declining after 30 min for all cells. We therefore fitted only the later time points with a single exponential, allowing the amplitude at $t = 35$ min, $N(35)$, to be a free parameter as well.

$$N(t) = N(35)e^{-K_3 \cdot (t-35)} \quad (7')$$

This did not in any way affect the determination of the removal rate, and the decay of fluorescence was consistent with retinol being fully removed at later times in this case as well.

The dependence of the retinol removal rate on IRBP concentration was analyzed with a Michaelis kinetic scheme. If V_0, $V([I])$, and V_{max} are the removal rate in the absence of any carriers, at IRBP concentration $[I]$, and at saturating concentrations of IRBP, respectively, then

$$V([I]) = V_0 + V_{max}[I]/([I] + K_I) \quad (8)$$

where K_I is the IRBP concentration resulting in the half-maximal removal rate. Equation 8 can be derived from a simplified scheme for retinol removal that involves an IRBP receptor, R, on the rod outer segment plasma membrane, with apparent affinity constant K_I for IRBP

$$R + IRBP \overset{K_I}{\leftrightarrow} R \cdot IRBP \quad (9a)$$

with retinol being removed at rate r according to

$$R \cdot IRBP + \text{retinol} \xrightarrow{r} R + IRBP \cdot \text{retinol} \quad (9b)$$

giving the following equation.

$$d[ROL]/dt = -r[R \cdot IRBP]ROL \quad (9c)$$

Assuming equilibrium between the IRBP and the receptor and substituting into eq 9c, we have

$$d[ROL]/dt = -r[R]_T \cdot K_I\{[I]/([I] + K_I)\}ROL \quad (10)$$

with R_T the total concentration of receptor on the plasma membrane. After taking into account the carrier-independent removal of retinol proceeding with rate V_0, eq 8 follows from eq 10 with $V_{max} = r[R]_T \cdot K_I$.

The kinetics of formation and removal of all-*trans* retinol in the outer segments of intact frog rod photoreceptors were analyzed according to the scheme of eq 1, using the independently determined parameters for steps *A*, *B*, and *C*. The concentration of retinol, $ROL(t)$ in the outer segment after rhodopsin bleaching is given by

$$ROL(t) = \beta \cdot P_0(X \cdot e^{-k_1 t} + Y \cdot e^{-k_2 t} + Z \cdot e^{-K_3 t}) \quad (11)$$

with

$$X = A_1 \cdot k_1/(K_3 - k_1) \quad (12a)$$

$$Y = A_2 \cdot k_2/(K_3 - k_2) \quad (12b)$$

$$Z = -(X + Y) \quad (12c)$$

The parameters A_1, A_2, k_1, and k_2 characterize the release of all-*trans* retinal (step *A* and eq 2 above), parameter β is the fraction of released retinal converted to retinol (step *B* and eq 4), and parameter K_3 characterizes the removal of all-*trans* retinol (step *C* and eq 7). P_0 is the concentration of

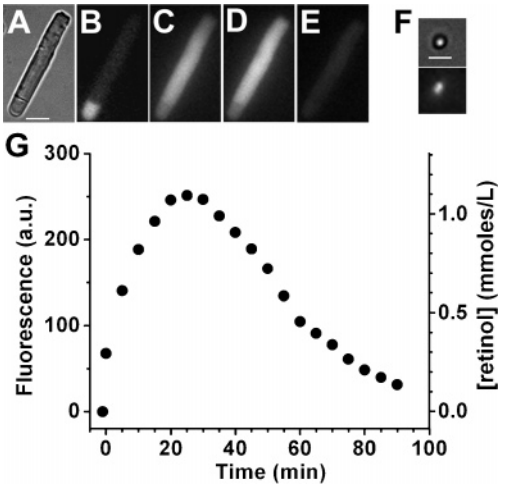

FIGURE 1: Formation and removal of all-*trans* retinol in an isolated frog rod photoreceptor in the presence of physiological concentrations of lipophilic carriers, IRBP (7 μmol/L) and BSA (3 μmol/L). (A) Infrared image of the dark-adapted rod cell. The bar is 10 μm. (B−E) Fluorescence images (excitation, 360 nm; emission, >420 nm) of the cell at different time points after bleaching. Images C−E are shown at the same fluorescence intensity scaling. (B) Dark-adapted cell, before bleaching; (C) 10 min after bleaching of rhodopsin for 1 min; (D) 30 min after bleaching; (E) 90 min after bleaching. (F) Bright field and fluorescence images of a hexane/chloroform droplet containing 435 μmol/L all-*trans* retinol. The bar is 5 μm. The relationship between fluorescence and concentration from such droplets was used to convert outer segment retinol fluorescence to concentration. (G) Rod outer segment retinol fluorescence and concentration at different times after bleaching the outer segment complement of rhodopsin. Bleaching was carried out between $t = -1$ min and $t = 0$. See text for details.

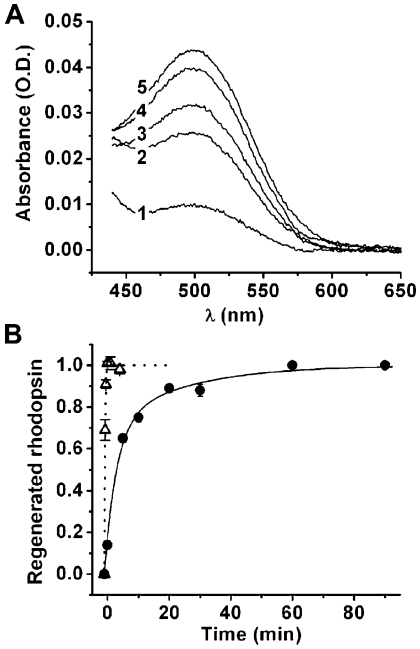

FIGURE 2: Measurement of the kinetics of all-*trans* retinal release from bleached frog rhodopsin in rod outer segment membranes. Immediately after bleaching, a large excess of 11-*cis* retinal is added, and as all-*trans* retinal is released new rhodopsin forms. (A) Absorbance spectra of rhodopsin recorded immediately (curve 1), 5 (curve 2), 10 (curve 3), 30 (curve 4), and 90 min (curve 5) after bleaching and adding 11-*cis* retinal. (B) Kinetics of rhodopsin regeneration after bleaching, reflecting the release of all-*trans* retinal (●, $n = 4$). Rhodopsin bleaching was carried out between $t = -1$ min and $t = 0$, and 11-*cis*-retinal was added immediately afterward. Data have been normalized to the level of rhodopsin regenerated after 90 min. The solid line curve is a two-exponential least-squares fit with amplitudes and rate constants 0.71 and 0.26 min^{-1}, and 0.29 and 0.04 min^{-1}, respectively. Regeneration of frog opsin with 11-*cis* was much faster (△, $n = 4$). The dotted line curve is a single-exponential curve fit with a rate constant of 4.74 min^{-1}.

rhodopsin present in outer segments. For *Rana pipiens* rod outer segments, $P_0 = 2.5$ mmol/L (*27*).

RESULTS

The bleaching of rhodopsin in photoreceptor rod outer segments of a variety of vertebrate species results in a gradual increase of fluorescence (*22*, *23*) that has been established to be due to all-*trans* retinol (*23*). Figure 1 shows an experiment with an isolated frog rod photoreceptor cell in the presence of 7 μmol/L IRBP and 3 μmol/L BSA, which correspond to the concentrations of the homologous proteins reported to be present in the frog interphotoreceptor matrix (IPM; (*11*)). The cell was exposed for 1 min to light >530 nm, which was sufficient to bleach virtually all of the outer segment rhodopsin. Following bleaching, the rod outer segment fluorescence transiently increased and then declined (Figure 1G). The initial, pre-bleach outer segment fluorescence was subtracted from all subsequent values, providing the time-course of the fluorescence change specifically due to retinol. The retinol fluorescence was converted to concentration using the fluorescence of chloroform/hexane droplets that contained a known concentration of retinol (435 μmol/L) (Figure 1F) and correcting for the difference in diameters of outer segment and droplet (see Materials and Methods). The calculated retinol concentration corresponding to the fluorescence values is shown on the right *y*-axis in Figure 1G.

We have separately characterized the two processes that underlie the retinol concentration changes observed in such experiments. One process is the formation of all-*trans* retinol from the all-*trans* retinal released from photoactivated rhodopsin, and the other is the removal of all-*trans* retinol by the lipophilic carriers IRBP and BSA present in the solution surrounding the cell. We first characterized the release of all-*trans* retinal from photoactivated rhodopsin in frog rod outer segment membranes by measuring the appearance of empty opsin sites. The concentration of empty sites was assessed through the concentration of regenerated rhodopsin by adding a large excess of 11-*cis* retinal immediately after bleaching. The concentration of regenerated rhodopsin was measured in the presence of hydroxylamine, which eliminated any spectral inteference from rhodopsin photointermediates: contrary to rhodopsin, which is stable in hydroxylamine and absorbs maximally in the 500 nm region, the chromophore−protein bond in the photointermediates is sensitive to hydroxylamine and gives rise to retinal oxime, which absorbs in the 360 nm region. Figure 2A shows the progressive increase with time in the amount of newly formed rhodopsin after bleaching frog rod outer segment membranes for 1 min with light >530 nm and adding an excess of 11-*cis* retinal. Figure 2B shows the kinetics of all-*trans* retinal release from photoactivated rhodopsin, measured as regenerated rhodopsin (●, $n = 4$). The release of all-*trans* retinal was described according to eq 2 as the sum of two first-order processes with relative amplitudes $A_1 = 0.71$ and $A_2 = 0.29$ and corresponding rate

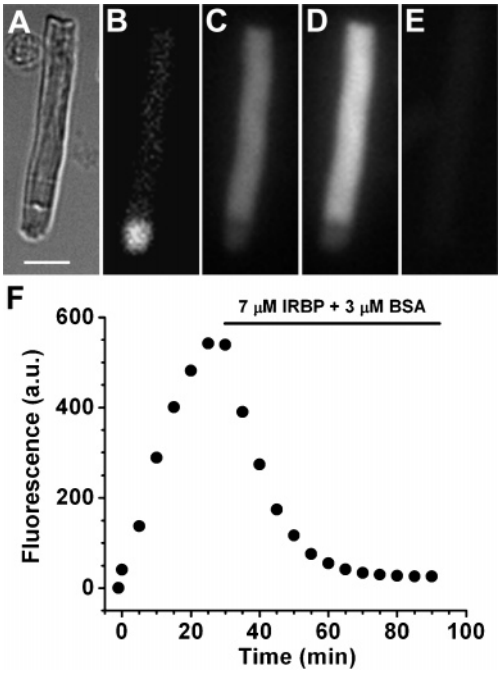

FIGURE 3: Measurement of all-*trans* retinol removal by physiological concentrations of lipophilic carriers. (A) Infrared image of the dark-adapted rod cell. The bar is 10 μm. (B−E) Fluorescence images (excitation, 360 nm; emission, >420 nm) of the cell at different time points after bleaching. Images C−E are shown at the same fluorescence intensity scaling. (B) Dark-adapted cell, before bleaching; (C) 10 min after bleaching of rhodopsin for 1 min; (D) 30 min after bleaching, just before the addition of lipophilic carriers; (E) 90 min after bleaching. (F) Rod outer segment retinol fluorescence at different times after bleaching the outer segment complement of rhodopsin. Bleaching was carried out between $t = -1$ min and $t = 0$. Physiological concentrations of IRBP (7 μmol/L) and BSA (3 μmol/L) were added to the solution, bathing the cell at $t = 30$ min.

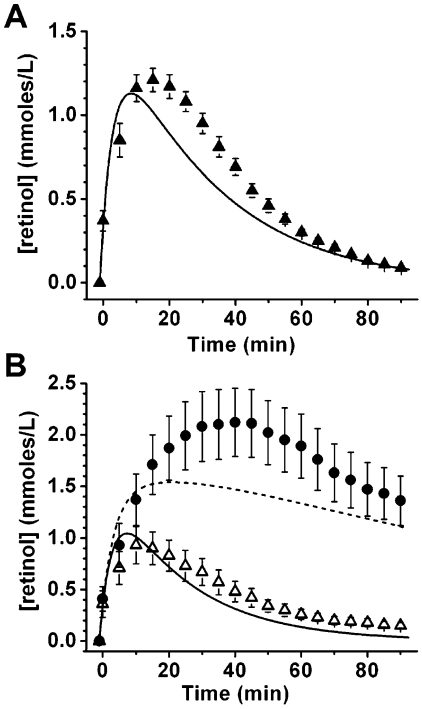

FIGURE 4: Comparisons of the experimentally measured timecourse of all-*trans* retinol concentration after rhodopsin bleaching with model predictions based on independently measured all-*trans* retinal release and all-*trans* retinol removal. The models assume thermodynamic equilibrium between retinal and retinol. The experimental data are from isolated frog rod photoreceptors. (A) Time course of all-*trans* retinol concentration after rhodopsin bleaching in the presence of physiological concentrations of lipophilic carriers (▲, $n = 16$) and the corresponding model (solid line). (B) Time course of all-*trans* retinol concentration after rhodopsin bleaching in the absence of lipophilic carriers (data: ●, $n = 14$; model: dotted line) and in the presence of 150 μmol/L BSA (data: △, $n = 14$; model: solid line). The error bars represent standard errors.

constants $k_1 = 0.26$ min^{-1} and $k_2 = 0.04$ min^{-1}. The amplitudes and rate constants were determined by a least-squares fit of eq 2 to the experimental data points. The reaction between 11-*cis* retinal and opsin (Figure 2B, △, $n = 4$) proceeded more than 10× faster and therefore was not a limiting factor in the determination of the kinetics of all-*trans* retinal release.

The removal of all-*trans* retinol was characterized by exposing isolated rods to physiological concentrations of lipophilic carriers (7 μmol/L IRBP and 3 μmol/L BSA (*11*)) beginning 30 min after the bleaching of rhodopsin. The removal of retinol was then followed through the decline of its outer segment fluorescence. Figure 3 shows such an experiment, in which the concentrations of carriers found in the frog interphotoreceptor matrix were added 30 min after bleaching. Upon the addition of carriers, retinol fluorescence declined (Figure 3F). The decline was described as a first-order process (eq 7), resulting in a removal rate constant of 0.073 min^{-1}. The average removal rate was 0.042 ± 0.009 min^{-1} ($n = 6$).

Given the kinetics of all-*trans* retinal release from photoactivated rhodopsin and the rate of all-*trans* retinol removal, and assuming rapid equilibration of retinal and retinol, the scheme shown in eq 1 provides the basis for the calculation of the expected time course of the change in retinol concentration in the outer segment after the bleaching of rhodopsin. The time course was calculated according to eq 11 and is compared to the experimental data in Figure 4A. We judge the agreement to be fairly reasonable because the discrepancy is much less than the cell-to-cell variability. To provide a sense of the variability from cell to cell, the peak concentration of outer segment retinol ranged from 0.9 to 2.3 mmol/L. We interpret this variability to arise from differences in the intracellular environment, including, for example, metabolic activity and pH, factors that directly affect the formation of retinol. We carried out comparisons between experimental data and model predictions under two additional conditions: in the absence of any lipophilic carriers and in the presence of 150 μmol/L BSA. These conditions affect the removal rate of all-*trans* retinol (step *C* in eq 1) but should leave the other steps unaffected. The rate of retinol removal in the absence of carriers was 0.007 min^{-1} and in the presence of 150 μmol/L BSA was 0.056 min^{-1} (see Figure 6). Figure 4B compares the model calculations with experimental data obtained under the two conditions. The range of peak retinol concentrations in the absence of carriers was 0.7 to 4.5 mmol/L and in the presence of 150 μmol/L of BSA 0.3 to 2.5 mmol/L. Therefore, again, there is very good agreement between the model predictions and the experimental results.

This good agreement suggested that the assumption of rapid equilibrium between all-*trans* retinal and retinol is approximately correct. We have independently tested this possibility by measuring the formation of all-*trans* retinol

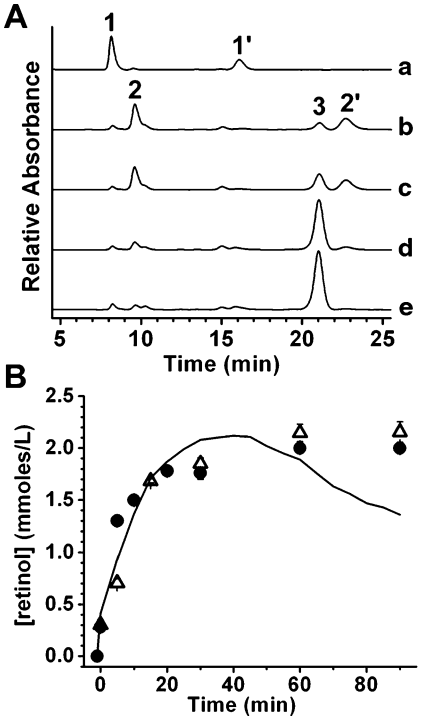

FIGURE 5: Direct comparison of the kinetics of all-*trans* retinal release and all-*trans* retinol formation in frog rod photoreceptors. (A) Chromatographic profiles (at 325 nm) of retinoid extractions from frog retinas, incubated for different times at room temperature after the bleaching of rhodopsin for 1 min; a, dark control; b, immediately after bleaching; c, 5 min; d, 30 min; e, 90 min after bleaching. 1, *syn*-11-*cis* retinal oxime; 1′, *anti*-11-*cis* retinal oxime; 2, *syn*-all-*trans* retinal oxime; 2′, *anti*-all-*trans* retinal oxime; 3, all-*trans* retinol. To allow comparisons, the traces have been normalized to the total amount of retinoid present in each sample (see Materials and Methods). (B) Comparison of the measured levels of all-*trans* retinol formed (△, extractions; —, fluoresence) after rhodopsin bleaching with the levels expected from the all-*trans* retinal released from rhodopsin (●) assuming that retinal and retinol are in thermodynamic equilibrium. There is good agreement between the kinetics of all-*trans* retinol formation measured with the two different techniques. There is also agreement between the measured kinetics of all-*trans* retinol formation with those expected from all-*trans* retinal release, suggesting that the release of all-*trans* retinal from the bleached pigment controls the kinetics of retinol formation. See text for details.

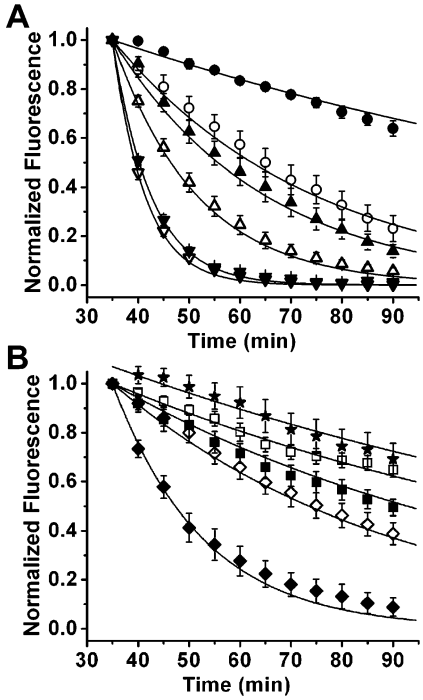

FIGURE 6: Measurement of the rates of all-*trans* retinol removal from frog rod outer segments by different concentrations of lipophilic carriers. Different concentrations of carriers were added 30 min after the bleaching of rhodopsin. Retinol outer segment fluorescence intensities have been normalized over the value at 35 min. Symbols represent experimental data points. The lines are simple exponentials, $e^{-K_3\cdot(t-35)}$, with unitary amplitude at $t = 35$ min, and decaying to 0, drawn with rate constants K_3 determined from the individual cells. (A) Removal of all-*trans* retinol by different concentrations of IRBP. IRBP concentrations and removal rates are in μmol/L and min^{-1}, respectively: 1, 0.007 ± 0.001 (●, $n = 10$); 3, 0.025 ± 0.004 (○, $n = 7$); 7, 0.034 ± 0.004 (▲, $n = 7$); 20, 0.061 ± 0.007 (△, $n = 10$); 50, 0.133 ± 0.009 (▼, $n = 7$); and 150, 0.158 ± 0.012 (▽, $n = 12$). (B) Removal of all-*trans* retinol by different concentrations of BSA. BSA concentrations and removal rates are in μmol/L and min^{-1}, respectively: 0, 0.007 ± 0.001 (★, $n = 14$); 3, 0.008 ± 0.001 (not shown, $n = 7$); 7, 0.009 ± 0.001 (□, $n = 9$); 20, 0.011 ± 0.002 (■, $n = 7$); 50, 0.020 ± 0.002 (◇, $n = 6$); and 150, 0.056 ± 0.008 (♦, $n = 6$). The exponential decay curve for the control cell data (no carriers) has been drawn with an amplitude of 1.07 (see text for additional details). The error bars represent standard errors.

with quantitative HPLC of retinoid extracts and comparing it with the release of all-*trans* retinal. Figure 5A shows chromatograms of retinoid extracts from frog retinas incubated for different times after light exposure. The concentration of all-*trans* retinol that forms after bleaching was calculated from such chromatograms and plotted as a function of time in Figure 5B (△, $n = 4$). All-*trans* retinal is released at essentially the same rate (Figure 2B). Thus, the concentration of released retinal converted to retinol at thermodynamic equilibrium (79% from eq 4; ● in Figure 5B) is in close agreement with the concentration of formed retinol. The concentration of formed retinol as measured by fluorescence (● in Figure 4B; — in Figure 5B) is also in good agreement with the HPLC measurements and the retinal release measurements. The slow decline of fluorescence with time is due to the slow removal of retinol from the outer segments of isolated cells.

The removal of retinol was examined in more detail by exposing cells to different concentrations of carriers. Carriers were added to the solution, bathing a cell 30 min after the bleaching of rhodopsin, and the removal of retinol was followed through the decline of outer segment fluorescence (for a specific example, see Figure 3). At high concentrations of IRBP (50 and 150 μmol/L), the outer segment fluorescence declined to its pre-bleach value, suggesting that retinol was removed completely. The fluorescence decline for each cell was analyzed according to eq 7, and the averaged data are plotted in Figure 6. The solid lines through the experimental data points are simple exponentials, $e^{-K_3\cdot(t-35)}$, with unitary amplitude at $t = 35$ min, and decaying to 0, consistent with retinol being fully removed at late times. The rate constant, K_3, for each curve is the average of the rate constants obtained from each cell for the particular carrier concentration. In the absence of lipophilic carriers, the retinol fluorescence in some cells kept increasing after 35 min. In these cases, eq 7′ was used to obtain the removal rate. The exponential decay curve for the control cells (symbol ★ in Figure 6B) has been drawn with an amplitude of 1.07 to take into account this difference in data processing.

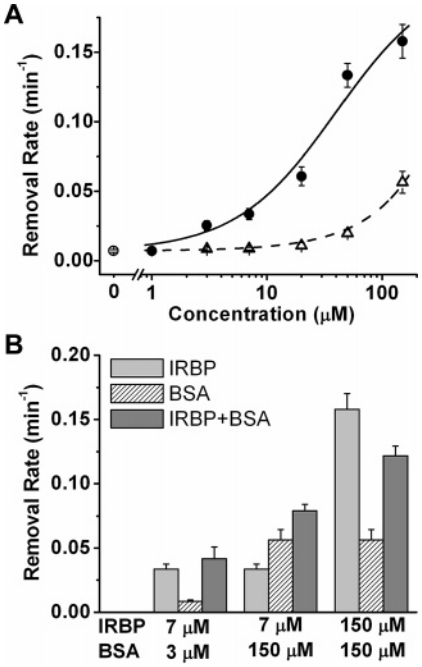

FIGURE 7: Dependence of the rate of retinol removal on the concentration of lipophilic carriers. (A) Average rate of retinol removal as a function of IRBP (●) and BSA (△) concentrations. The rate in the absence of carriers (○) was $V_0 = 0.007 \pm 0.001$ min^{-1}. The data are from the experiments shown in Figure 5. The errors bars represent standard errors. The solid line is a least-squares fit for the effect of IRBP, according to eq 8 giving $K_I = 40$ μmol/L and $V_{max} = 0.20$ min^{-1}. The dashed line is a linear least-squares fit, with a slope of 0.00032 min^{-1}/(μmol BSA/L). (B) Removal of retinol by different combinations of IRBP and BSA. The contribution of the physiological BSA concentration (3 μmol/L) to the removal of retinol is negligible, whereas high concentrations of BSA interfere with the removal of retinol by IRBP.

The effect of IRBP on the removal rate of retinol saturates at higher concentrations, as can be seen from the similarity of the effects of 50 (▼) and 150 μmol/L (▽) in Figure 6A. In contrast, the effect of BSA keeps increasing with concentration, not showing any signs of saturation (Figure 6B). Figure 7 shows the dependence of the rate of retinol removal on carrier concentration. The effect of IRBP shows an EC_{50} of 40 μmol/L and no significant cooperativity. The effect of BSA increases linearly with concentration, with a slope of 0.00032 min^{-1}/(μmol/L). It is possible that the effect of BSA might saturate at higher concentrations, but even in that case the EC_{50} would be in the order of mmol/L, too high for a specific protein−protein interaction. The data are consistent with a specific interaction between IRBP and the rod outer segment plasma membrane, whereas the effect of BSA is nonspecific. We probed the possibility of an interaction between IRBP and BSA by testing whether their effects are additive. We carried out this test at three different combinations of concentrations of IRBP and BSA (in μmol/L): 7 and 3 giving $K_3 = 0.042 \pm 0.009$ min^{-1} ($n = 6$), 7 and 150 giving $K_3 = 0.079 \pm 0.005$ min^{-1} ($n = 10$), and 150 and 150 giving $K_3 = 0.122 \pm 0.008$ min^{-1} ($n = 12$) (Figure 6B). When considering the physiological concentrations of carriers, the difference between the effect of the combination of 7 μmol/L IRBP and 3 μmol/L BSA, 0.042 ± 0.009 min^{-1}, was not significantly different from the effect of 7 μmol/L IRBP alone, 0.034 ± 0.004 min^{-1} (one-way ANOVA, $p = 0.41$). However, 150 μmol/L BSA strongly interfered with the removal of retinol by 150 μmol/L IRBP (one-way ANOVA, $p = 0.02$). This interference by BSA excludes the possibility that the carriers speed up the removal of retinol by virtue of increasing its effective solubility. It also suggests that there is some overlap of the paths via which IRBP and BSA remove retinol.

DISCUSSION

The good agreement shown in Figure 4 between the experimental data and the predictions from the model described by eq 11 suggests that the simplified model of eq1 provides a good first approximation to the process of all-*trans* retinol formation and clearance. A central assumption in this simple model is that the reduction reaction of retinal to retinol by the retinol dehydrogenase (eq 3 and step *B* in eq1) is in rapid equilibrium. The agreement between the model and the experimental data would indicate that this assumption is largely correct and that the release of all-*trans* retinal from photoactivated rhodopsin is limiting in the formation of all-*trans* retinol. This is corroborated by the close agreement between the kinetics of retinal release and retinol formation (Figure 5B).

The rate of all-*trans* retinal release depends on several factors. The release of all-*trans* retinal occurs after the hydrolysis of the chromophore−protein bond, which is the last step in a sequence of conformational changes initiated by the photoisomerization of the retinyl moiety from 11-*cis* to all-*trans*. The overall kinetics of rhodopsin photochemistry are highly dependent on temperature, pH, and the membrane environment (*38*−*40*). We have approximated physiological conditions using frog rod outer segment membranes, a high K^+ buffer, and a pH of 7.3 that reflects the intracellular outer segment pH, without, however, being able to mimic the asymmetry provided by the disk topology that gives rise to separate intradiskal and cytoplasmic spaces. The kinetics of retinal release reported here are largely consistent with previous measurements on frog rhodopsin (but at 15 °C (*41*)), with the decay of the photoproducts metarhodopsin II and III (*40*, *42*, *43*), and with microspectrophotometry of intact frog rod photoreceptors (*44*). They are also in broad agreement with the kinetics measured from the increase in rhodopsin tryptophan fluorescence associated with retinal release (*43*, *45*). Other factors that can affect the release of all-*trans* retinal involve the enzymes responsible for the deactivation of photoactivated rhodopsin. The deactivation of light-activated rhodopsin involves phosphorylation by rhodopsin kinase followed by the binding of arrestin. Experiments *in vitro* have suggested that arrestin binding to phosphorylated photoactivated rhodopsin slows the release of all-*trans* retinal (*46*, *47*). The release of retinal we have measured is in the absence of added ATP; therefore, it would be from unphosphorylated photoactivated rhodopsin. The close agreement between the kinetics of retinal release and retinol formation would indicate that at least to a first approximation and at high bleaches the presence of arrestin does not appear to affect the rate of retinal release from photoactivated rhodopsin.

After its release from rhodopsin, some of the all-*trans* retinal can be sequestered inside the disks, bound via a Schiff base to phosphatidylethanolamine(*9*). The phosphatidylethanolamine-all-*trans* retinal compound can then be transported

to the cytoplasmic side by the ABCR transporter so that all-*trans* retinal becomes available for reduction by the dehydrogenase (*8*−*10*). Again, the close agreement between the kinetics of all-*trans* retinal release and of retinol formation suggests that any sequestration of all-*trans* retinal does not place a significant limit on the delivery of retinol to the dehydrogenase.

Another important implication of the agreement between the kinetics of retinal release and of retinol formation is that it suggests that the reduction reaction itself is not limiting. This suggests that both the supply of NADPH and the catalytic activity of the retinol dehydrogenase can keep up with the release of retinal from photoactivated rhodopsin. NADPH can be supplied by the hexose monophosphate shunt operating in the rod outer segments (*48*) and also by additional pathways (*49*), as evidenced by the difficulty in suppressing retinol formation with metabolic inhibitors (*23*). It seems then that frog rod photoreceptors can rapidly supply the necessary reducing equivalents for the conversion of all-*trans* retinal to retinol, in agreement with the microspectrophotometric observations of the fast appearance of retinol after all-*trans* retinal release (*44*). This contrasts with salamander photoreceptors, in which case it appears that NADPH can become limiting in the distal parts of the outer segment, leading to a spatial gradient in the formation of retinol (*22*, *24*). Such gradients are rarely observed in frog rods. The kinetics of retinol formation presented here are also in agreement with the spectroscopic measurements of Baumann (*50*) in perfused frog retinas.

Because retinol has a small aqueous solubility (*51*), it can leave the outer segment even in the absence of lipophilic carriers. As previously observed in salamander photoreceptors (*22*, *24*), both IRBP and BSA can facilitate the removal of all-*trans* retinol. Virtually all of the retinol can be removed, in accordance with the bulk of it being free (*28*). Both IRBP and BSA bind retinol, although the latter does so with an order of magnitude lower affinity (*52*, *53*). Moreover, both of them retain a large fraction of any loaded retinol (*54*), and therefore, it is conceivable that they can facilitate the removal of retinol through an increase of its effective solubility. However, the large difference in effectiveness between IRBP and BSA, much larger than their small difference in retinol-retaining capacity (*54*), argues strongly against such a mode of action. In addition, the interference by high concentrations of BSA on the removal by IRBP is inconsistent with such a nonspecific increase in bulk solubility. Instead, the data are consistent with the removal of retinol by IRBP being mediated by a specific interaction with the rod outer segment plasma membrane, a possibility supported by the observed close association of IRBP with the photoreceptor plasma membrane (*55*, *56*). A simple mechanism would be a receptor protein for IRBP, whereas the interfering effect by BSA could be due to nonspecific masking of the rod outer segment plasma membrane at high concentrations. A specialized interaction between IRBP and the rod outer segment plasma membrane has also been suggested by experiments measuring the recovery of bleached photoreceptor cell sensitivity upon delivery of 11-*cis* retinal (*57*). There is a difference in the kinetics of sensitivity recovery with IRBP as the carrier of 11-*cis* retinal compared to that with liposomes as the carrier (*57*). The half-saturation concentration and the lack of cooperativity for the IRBP effect suggest that IRBP binds to the putative receptor one-to-one with an affinity $K_I = 40$ μmol/L (eqs 8−10). The observed EC_{50} cannot reflect the binding of retinol by IRBP, as this affinity is much higher, ~180 nmol/L (*53*).

Although the IRBP and serum albumin proteins that we have used are from bovine, the mammalian and amphibian IRBPs are homologous (*58*, *59*). This is particularly relevant in considering the implications of the results for the physiological concentrations of the carriers. Adler and Edwards (*11*) have reported that the concentrations of IRBP and serum albumin in the frog IPM are 7 and 3 μmol/L, respectively. We have found that these concentrations can efficiently remove the accumulating retinol (Figures 1 and 3), and the contribution of 3 μmol/L albumin is negligible (Figure 7). More generally, our results (Figure 7A) suggest that the effect of serum albumin becomes significant above 50 μmol/L, whereas the highest reported concentration in the IPM is 28 μmol/L (for humans; (*11*)). In addition, recent experiments have found no evidence for the presence of serum albumin in the IPM (*56*, *60*). Our results would then suggest that even in the presence of the reported concentrations in the IPM serum albumin does not contribute significantly to the removal of retinol, and therefore, IRBP is the physiologically relevant carrier of retinol in the IPM.

The rapid removal of retinol facilitated by IRBP speeds up the clearance of all-*trans* retinal. Retinal, apart from being a reactive aldehyde, can also act as a photosensitizer (*61*, *62*) because its absorption spectrum (λ_{max} ~380 nm) extends into the visible range. For the whole animal, the efficient clearance of retinal will be of particular relevance under bright light conditions when retinal will be generated continuously. In mice lacking IRBP, however, the Visual Cycle remains operational (*63*, *64*), suggesting that either another, yet unknown, carrier protein is involved or that the intermembranous transfer of retinol facilitated by the close apposition between the rod outer segment and RPE cell membranes suffices. It might well be the case that IRBP becomes physiologically relevant at high light intensities when large amounts of all-*trans* retinal and retinol are continuously generated.

ACKNOWLEDGMENT

We thank Dr. Mas Kono for helpful discussions.

REFERENCES

1. Ebrey, T., and Koutalos, Y. (2001) Vertebrate photoreceptors, *Prog. Retinal Eye Res. 20*, 49−94.
2. Fain, G. L., Matthews, H. R., Cornwall, M. C., and Koutalos, Y. (2001) Adaptation in vertebrate photoreceptors, *Physiol. Rev. 81*, 117−151.
3. Lamb, T. D., and Pugh, E. N., Jr. (2004) Dark adaptation and the retinoid cycle of vision, *Prog. Retinal Eye Res. 23*, 307−380.
4. McBee, J. K., Palczewski, K., Baehr, W., and Pepperberg, D. R. (2001) Confronting complexity: the interlink of phototransduction and retinoid metabolism in the vertebrate retina, *Prog. Retinal Eye Res. 20*, 469−529.
5. Saari, J. C. (2000) Biochemistry of visual pigment regeneration: the Friedenwald lecture, *Invest. Ophthalmol. Visual Sci. 41*, 337−348.
6. Futterman, S., Hendrickson, A., Bishop, P. E., Rollins, M. H., and Vacano, E. (1970) Metabolism of glucose and reduction of retinaldehyde in retinal photoreceptors, *J. Neurochem. 17*, 149−156.

7. Palczewski, K., Jager, S., Buczylko, J., Crouch, R. K., Bredberg, D. L., Hofmann, K. P., Asson-Batres, M. A., and Saari, J. C. (1994) Rod outer segment retinol dehydrogenase: substrate specificity and role in phototransduction, *Biochemistry 33*, 13741−13750.
8. Beharry, S., Zhong, M., and Molday, R. S. (2004) N-retinylidene-phosphatidylethanolamine is the preferred retinoid substrate for the photoreceptor-specific ABC transporter ABCA4 (ABCR), *J. Biol. Chem. 279*, 53972−53979.
9. Weng, J., Mata, N. L., Azarian, S. M., Tzekov, R. T., Birch, D. G., and Travis, G. H. (1999) Insights into the function of Rim protein in photoreceptors and etiology of Stargardt's disease from the phenotype in abcr knockout mice, *Cell 98*, 13−23.
10. Sun, H., Molday, R. S., and Nathans, J. (1999) Retinal stimulates ATP hydrolysis by purified and reconstituted ABCR, the photoreceptor-specific ATP-binding cassette transporter responsible for Stargardt disease, *J. Biol. Chem. 274*, 8269−8281.
11. Adler, A. J., and Edwards, R. B. (2000) Human interphotoreceptor matrix contains serum albumin and retinol-binding protein, *Exp. Eye Res. 70*, 227−234.
12. Okajima, T. I., Pepperberg, D. R., Ripps, H., Wiggert, B., and Chader, G. J. (1989) Interphotoreceptor retinoid-binding protein: role in delivery of retinol to the pigment epithelium, *Exp. Eye Res. 49*, 629−644.
13. Qtaishat, N. M., Wiggert, B., and Pepperberg, D. R. (2005) Interphotoreceptor retinoid-binding protein (IRBP) promotes the release of all-trans retinol from the isolated retina following rhodopsin bleaching illumination, *Exp. Eye Res. 81*, 455−463.
14. Batten, M. L., Imanishi, Y., Maeda, T., Tu, D. C., Moise, A. R., Bronson, D., Possin, D., Van Gelder, R. N., Baehr, W., and Palczewski, K. (2004) Lecithin-retinol acyltransferase is essential for accumulation of all-trans-retinyl esters in the eye and in the liver, *J. Biol. Chem. 279*, 10422−10432.
15. Saari, J. C., Bredberg, D. L., and Farrell, D. F. (1993) Retinol esterification in bovine retinal pigment epithelium: reversibility of lecithin:retinol acyltransferase, *Biochem. J. 291*, 697−700.
16. McBee, J. K., Kuksa, V., Alvarez, R., de Lera, A. R., Prezhdo, O., Haeseleer, F., Sokal, I., and Palczewski, K. (2000) Isomerization of all-trans-retinol to cis-retinols in bovine retinal pigment epithelial cells: dependence on the specificity of retinoid-binding proteins, *Biochemistry 39*, 11370−11380.
17. Bernstein, P. S., and Rando, R. R. (1986) In vivo isomerization of all-trans- to 11-cis-retinoids in the eye occurs at the alcohol oxidation state, *Biochemistry 25*, 6473−6478.
18. Jin, M., Li, S., Moghrabi, W. N., Sun, H., and Travis, G. H. (2005) Rpe65 is the retinoid isomerase in bovine retinal pigment epithelium, *Cell 122*, 449−459.
19. Moiseyev, G., Chen, Y., Takahashi, Y., Wu, B. X., and Ma, J. X. (2005) RPE65 is the isomerohydrolase in the retinoid visual cycle, *Proc. Natl. Acad. Sci. U.S.A. 102*, 12413−12418.
20. Redmond, T. M., Poliakov, E., Yu, S., Tsai, J. Y., Lu, Z., and Gentleman, S. (2005) Mutation of key residues of RPE65 abolishes its enzymatic role as isomerohydrolase in the visual cycle, *Proc. Natl. Acad. Sci. U.S.A. 102*, 13658−13663.
21. Redmond, T. M., Yu, S., Lee, E., Bok, D., Hamasaki, D., Chen, N., Goletz, P., Ma, J. X., Crouch, R. K., and Pfeifer, K. (1998) Rpe65 is necessary for production of 11-cis-vitamin A in the retinal visual cycle, *Nat. Genet. 20*, 344−351.
22. Tsina, E., Chen, C., Koutalos, Y., Ala-Laurila, P., Tsacopoulos, M., Wiggert, B., Crouch, R. K., and Cornwall, M. C. (2004) Physiological and microfluorometric studies of reduction and clearance of retinal in bleached rod photoreceptors, *J. Gen. Physiol. 124*, 429−443.
23. Chen, C., Tsina, E., Cornwall, M. C., Crouch, R. K., Vijayaraghavan, S., and Koutalos, Y. (2005) Reduction of all-trans retinal to all-trans retinol in the outer segments of frog and mouse rod photoreceptors, *Biophys. J. 88*, 2278−2287.
24. Ala-Laurila, P., Kolesnikov, A. V., Crouch, R. K., Tsina, E., Shukolyukov, S. A., Govardovskii, V. I., Koutalos, Y., Wiggert, B., Estevez, M. E., and Cornwall, M. C. (2006) Visual cycle: dependence of retinol production and removal on photoproduct decay and cell morphology, *J. Gen. Physiol. 128*, 153−169.
25. Liebman, P. A. (1969) Microspectrophotometry of retinal cells, *Ann. N.Y. Acad. Sci. 157*, 250−264.
26. Biernbaum, M. S., and Bownds, M. D. (1985) Frog rod outer segments with attached inner segment ellipsoids as an in vitro model for photoreceptors on the retina, *J. Gen. Physiol. 85*, 83−105.
27. Liebman, P. A., and Entine, G. (1968) Visual pigments of frog and tadpole (*Rana pipiens*), *Vision Res. 8*, 761−775.
28. Wu, Q., Chen, C., and Koutalos, Y. (2006) All-trans retinol in rod photoreceptor outer segments moves unrestrictedly by passive diffusion, *Biophys. J. 91*, 4678−4689.
29. Pepperberg, D. R., Okajima, T. L., Ripps, H., Chader, G. J., and Wiggert, B. (1991) Functional properties of interphotoreceptor retinoid-binding protein, *Photochem. Photobiol. 54*, 1057−1060.
30. Fung, B. K., Hurley, J. B., and Stryer, L. (1981) Flow of information in the light-triggered cyclic nucleotide cascade of vision, *Proc. Natl. Acad. Sci. U.S.A. 78*, 152−156.
31. Jager, S., Palczewski, K., and Hofmann, K. P. (1996) Opsin/all-trans-retinal complex activates transducin by different mechanisms than photolyzed rhodopsin, *Biochemistry 35*, 2901−2908.
32. Fan, J., Rohrer, B., Moiseyev, G., Ma, J. X., and Crouch, R. K. (2003) Isorhodopsin rather than rhodopsin mediates rod function in RPE65 knock-out mice, *Proc. Natl. Acad. Sci. U.S.A. 100*, 13662−13667.
33. Saari, J. C., Garwin, G. G., Van Hooser, J. P., and Palczewski, K. (1998) Reduction of all-trans-retinal limits regeneration of visual pigment in mice, *Vision Res. 38*, 1325−1333.
34. Furr, H. C., Barua, A. B., and Olson, J. A. (1994) Analytical Methods, in *Retinoids: Biology, Chemistry, and Medicine* (Sporn, M. B., Roberts, A. B., and Goodman, D. S., Eds.) pp 179−209, Raven Press, New York, NY.
35. Matschinsky, F. M. (1968) Quantitative histochemistry of nicotinamide adenine nucleotides in retina of monkey and rabbit, *J. Neurochem. 15*, 643−657.
36. Bliss, A. F. (1951) The equilibrium between vitamin A alcohol and aldehyde in the presence of alcohol dehydrogenase, *Arch. Biochem. 31*, 197−204.
37. Chen, C., Jiang, Y., and Koutalos, Y. (2002) Dynamic behavior of rod photoreceptor disks, *Biophys. J. 83*, 1403−1412.
38. Wiedmann, T. S., Pates, R. D., Beach, J. M., Salmon, A., and Brown, M. F. (1988) Lipid-protein interactions mediate the photochemical function of rhodopsin, *Biochemistry 27*, 6469−6474.
39. Mitchell, D. C., Straume, M., and Litman, B. J. (1992) Role of sn-1-saturated,sn-2-polyunsaturated phospholipids in control of membrane receptor conformational equilibrium: effects of cholesterol and acyl chain unsaturation on the metarhodopsin I in equilibrium with metarhodopsin II equilibrium, *Biochemistry 31*, 662−670.
40. Matthews, R. G., Hubbard, R., Brown, P. K., and Wald, G. (1963) Tautomeric forms of metarhodopsin, *J. Gen. Physiol. 47*, 215−240.
41. Baumann, C., and Zeppenfeld, W. (1981) Effect of pH on the formation and decay of the metarhodopsins of the frog, *J. Physiol. 317*, 347−364.
42. Vogel, R., Siebert, F., Zhang, X. Y., Fan, G., and Sheves, M. (2004) Formation of Meta III during the decay of activated rhodopsin proceeds via Meta I and not via Meta II, *Biochemistry 43*, 9457−9466.
43. Heck, M., Schadel, S. A., Maretzki, D., Bartl, F. J., Ritter, E., Palczewski, K., and Hofmann, K. P. (2003) Signaling states of rhodopsin. Formation of the storage form, metarhodopsin III, from active metarhodopsin II, *J. Biol. Chem. 278*, 3162−3169.
44. Kolesnikov, A. V., Golobokova, E. Y., and Govardovskii, V. I. (2003) The identity of metarhodopsin III, *Vis. Neurosci. 20*, 249−265.
45. Farrens, D. L., and Khorana, H. G. (1995) Structure and function in rhodopsin. Measurement of the rate of metarhodopsin II decay by fluorescence spectroscopy, *J. Biol. Chem. 270*, 5073−5076.
46. Sommer, M. E., Smith, W. C., and Farrens, D. L. (2005) Dynamics of arrestin-rhodopsin interactions: arrestin and retinal release are directly linked events, *J. Biol. Chem. 280*, 6861−6871.
47. Hofmann, K. P., Pulvermuller, A., Buczylko, J., Van Hooser, P., and Palczewski, K. (1992) The role of arrestin and retinoids in the regeneration pathway of rhodopsin, *J. Biol. Chem. 267*, 15701−15706.
48. Hsu, S. C., and Molday, R. S. (1994) Glucose metabolism in photoreceptor outer segments. Its role in phototransduction and in NADPH-requiring reactions, *J. Biol. Chem. 269*, 17954−17959.
49. Winkler, B. S. (1986) Buffer dependence of retinal glycolysis and ERG potentials, *Exp. Eye Res. 42*, 585−593.
50. Baumann, C. (1972) Kinetics of slow thermal reactions during the bleaching of rhodopsin in the perfused frog retina, *J. Physiol. 222*, 643−663.

51. Szuts, E. Z., and Harosi, F. I. (1991) Solubility of retinoids in water, *Arch. Biochem. Biophys. 287*, 297−304.
52. N'Soukpoe-Kossi, C. N., Sedaghat-Herati, R., Ragi, C., Hotchandani, S., and Tajmir-Riahi, H. A. (2007) Retinol and retinoic acid bind human serum albumin: stability and structural features, *Int. J. Biol. Macromol. 40*, 484−490.
53. Tschanz, C. L., and Noy, N. (1997) Binding of retinol in both retinoid-binding sites of interphotoreceptor retinoid-binding protein (IRBP) is stabilized mainly by hydrophobic interactions, *J. Biol. Chem. 272*, 30201−30207.
54. Edwards, R. B., and Adler, A. J. (2000) IRBP enhances removal of 11- cis-retinaldehyde from isolated RPE membranes, *Exp. Eye Res. 70*, 235−245.
55. Schneider, B. G., Papermaster, D. S., Liou, G. I., Fong, S. L., and Bridges, C. D. (1986) Electron microscopic immunocytochemistry of interstitial retinol-binding protein in vertebrate retinas, *Invest. Ophthalmol. Visual Sci. 27*, 679−688.
56. Duncan, T., Fariss, R. N., and Wiggert, B. (2006) Confocal immunolocalization of bovine serum albumin, serum retinol-binding protein, and interphotoreceptor retinoid-binding protein in bovine retina, *Mol. Vision 12*, 1632−1639.
57. Jones, G. J., Crouch, R. K., Wiggert, B., Cornwall, M. C., and Chader, G. J. (1989) Retinoid requirements for recovery of sensitivity after visual-pigment bleaching in isolated photoreceptors, *Proc. Natl. Acad. Sci. U.S.A. 86*, 9606−9610.
58. Gonzalez-Fernandez, F., Baer, C. A., Baker, E., Okajima, T. I., Wiggert, B., Braiman, M. S., and Pepperberg, D. R. (1998) Fourth module of Xenopus interphotoreceptor retinoid-binding protein: activity in retinoid transfer between the retinal pigment epithelium and rod photoreceptors, *Curr. Eye Res. 17*, 1150−1157.
59. Gelderman, M. P., Gonzalez-Fernandez, F., Baer, C. A., Wiggert, B., Chan, C. C., Vistica, B. P., and Gery, I. (2000) Xenopus IRBP, a phylogenetically remote protein, is uveitogenic in Lewis rats, *Exp. Eye Res. 70*, 731−736.
60. Liao, R., and Gonzalez-Fernandez, F. (2004) Albumin is not present in the murine interphotoreceptor matrix, or in that of transgenic mice lacking IRBP, *Mol. Vision 10*, 1038−1046.
61. Delmelle, M. (1978) Retinal sensitized photodynamic damage to liposomes, *Photochem. Photobiol. 28*, 357−360.
62. Krasnovsky, A. A., Jr., and Kagan, V. E. (1979) Photosensitization and quenching of singlet oxygen by pigments and lipids of photoreceptor cells of the retina, *FEBS Lett. 108*, 152−154.
63. Palczewski, K., Van Hooser, J. P., Garwin, G. G., Chen, J., Liou, G. I., and Saari, J. C. (1999) Kinetics of visual pigment regeneration in excised mouse eyes and in mice with a targeted disruption of the gene encoding interphotoreceptor retinoid-binding protein or arrestin, *Biochemistry 38*, 12012−12019.
64. Ripps, H., Peachey, N. S., Xu, X., Nozell, S. E., Smith, S. B., and Liou, G. I. (2000) The rhodopsin cycle is preserved in IRBP "knockout" mice despite abnormalities in retinal structure and function, *Vis. Neurosci. 17*, 97−105.

BI7004619